

Two-dimensional versus three-dimensional behavior of a free-carrier gas in δ -doped p -type GaAs(001)

R. Biagi and U. del Pennino

Dipartimento di Fisica, Università di Modena, via G. Campi 213/A, I-41100 Modena, Italy

(Received 21 April 1994)

The free-carrier-induced plasma excitation in δ -doped p -type GaAs(001) has been studied by means of high-resolution electron-energy-loss spectroscopy (HREELS). Several samples, with different values of doping and depth of the dopant layer, have been investigated at various primary-beam energies. The HREEL spectra show a strong dependence on the doping level. We were able to reproduce satisfactorily all the measured spectra using a suitable dielectric model of a classically confined free-carrier gas, pointing out the two-dimensional character of the free-carrier gas in the samples having the two lowest dopings. On the contrary, a characteristic three-dimensional behavior of the plasma excitation is exhibited by the most doped sample.

I. INTRODUCTION

Recently, interest in the study of low-dimensional systems has grown considerably and has been motivated not only by the basic physics, connected to their characteristic electronic properties, but also by the technological applications, like quantum devices.^{1,2} "Classical" examples of such low-dimensional systems are the accumulation layer obtained in metal-oxide-semiconduction (MOS) structures¹ or at the surface of semiconductors like ZnO (Refs. 3 and 4) or InAs.⁵⁻⁷ The advent of the technique of epitaxial growth allowed the building of new kinds of such structures having interesting properties. In particular, the advances of molecular-beam epitaxy (MBE) allowed us to control the growth of the structure at the atomic-layer level, so that by interrupting and restarting the semiconductor growth after a planar doping, one can obtain the so-called δ -doped structure, in which the dopants are confined within a few monolayers.⁸ The ideal δ -doped structure, where only one atomic layer is doped, has not yet been achieved in the practice. Measurements of capacitance-voltage (C - V),⁹ magnetotransport,¹⁰ and secondary-ion-mass spectroscopy (SIMS) (Refs. 11 and 12) showed that the diffusion of the doping impurities (e.g., Si and Be in GaAs) occurs in a region of at least 20–30 Å, even at the lowest growth temperatures.

In these systems, carriers released by the dopants are confined inside the potential well setup by the ionized impurities. The spatial extension of this potential well and of the free-carrier gas can be determined by solving self-consistently the Schrödinger and Poisson equations.^{8,13} Since this extension is comparable to the de Broglie length of the carriers, the carrier motion is quantized along the normal to the dopant plane (z direction), while in the x - y plane the motion is free. The system, therefore, is, quasi-two-dimensional (2D), and the electronic structure is characterized by discrete levels (subbands). The electronic structure depends on the spatial distribution of the dopants, provided its extension is comparable to the width of the potential well.^{13,14} In these systems

the 2D behavior is retained up to a spatial extension of the gas by several hundreds Å. Above this value a transition from 2D to a 3D behavior occurs, as shown theoretically by Poole *et al.*¹⁵ and experimentally by Sernelius *et al.*¹⁶ for a metal-insulator-semiconductor (MIS) structure.

The dimensionality of the free-carrier gas is reflected by its collective excitation. An ideal 2D gas is characterized by a so-called acoustical dispersion of the collective excitations; that is, the plasmon frequency goes to zero when the wave vector $q_{\parallel} \rightarrow 0$,¹⁷ while in a 3D gas this frequency always retains a nonzero value.

The collective excitations in a 3D system have been widely studied by means of high-resolution electron-energy-loss spectroscopy (HREELS) (Refs. 18–20) and Raman spectroscopy,¹⁸ while in a single 2D electron gas (2DEG) they have been investigated much less.

Recently Lohe *et al.*¹⁹ presented a HREELS investigation on n -type δ -doped GaAs(001) samples in which the spectra were fairly well reproduced using a dielectric model, also accounting for some dopant diffusion.

In the present work we studied, by means of HREELS, the collective excitations (plasmons) of the free-carrier gas produced by a p -type layer of dopants (Be), embedded in GaAs(001) substrates many tens of Å under the surface, with three different charge densities. In particular, we wanted to check the dimensionality of the free-carrier gas in the different conditions, by means of its response to the electronic excitation. From the results of our measurements it comes out that the samples corresponding to the two lowest charge densities show expected 2D behavior, while the doped samples show a highly clear 3D behavior. Moreover, by means of a suitable dielectric modellization of the system we could extract the value of the plasma damping, showing that in the sample with intermediate doping ($3 \times 10^{13} \text{ cm}^{-2}$) it strongly increases with the plasmon wave vector. The paper is organized as follows: after the description of the experimental details (Sec. II), in Sec. III we present the results and in Sec. IV we discuss the quasi-2D excitation spectrum and the

models we assumed to calculate the theoretical spectra. In Sec. V we discuss the experimental spectra in comparison with the calculated ones, summarizing our conclusions in Sec. VI.

II. EXPERIMENT

Experiments were carried out at the surface physics laboratory SESAMO, Dipartimento di Fisica, Università di Modena. The HREELS spectrometer (Leybold-Heraeus ELS-22) is contained in an UHV as a system also equipped with low-energy electron diffraction (LEED), Auger electron spectroscopy (AES), ultraviolet photoemission spectroscopy (UPS), x-ray, and other auxiliary photoemission spectroscopy (XPS) facilities for sample preparation. Base pressure was below 7×10^{-11} mbar (7×10^{-9} Pa).

The δ -doped p -type samples were grown in the TASC-INFM Laboratory in Trieste by the MBE technique. Several samples, with different values of doping and depth under the surface of the dopant layer, were grown and analyzed (see Table I). In a typical preparation, on a GaAs(001) wafer (n^+ doped $\sim 10^{18}$ cm $^{-3}$) was grown a buffer layer of GaAs, lightly p -type doped (1×10^{16} cm $^{-3}$) and about 5000 Å thick, then, keeping the Ga and As shutters closed, only Be was evaporated to obtain a layer of dopant atoms. Finally, the growth of the lightly p -doped GaAs layer was started again. The growth temperature was about 580°C. The nominal doping densities were 3×10^{12} , 3×10^{13} , and 1×10^{14} cm $^{-2}$. In order to preserve the sample surface from contamination during the transfer of the samples to the analysis chamber, they were capped with a layer of amorphous As about 2000 Å thick, before breaking the ultrahigh vacuum. Once transferred inside the analysis chamber, the samples were decapped simply by heating at a temperature of about 350°C. After the As-cap desorption, the surface was perfectly mirrorlike and low-energy electron diffraction (LEED) showed a clear 1×1 pattern superimposed on a weak background. The cleanliness of the surface was monitored by means of HREELS and AES. We found a slight C and O contamination that we believe does not affect the results of our measurements, because the excitations investigated are localized deep under the surface (many tens of Å). In the case of the clean cleaved GaAs(110) surface the exposure to hydrogen or residual gas severely affects the surface by producing band bending.²⁰ On the clean GaAs(001) surface, however, the Fermi level is already pinned by the intrinsic surface states. Thus it is not affected by the contamination, as confirmed

TABLE I. Doping level and depth of the different samples investigated in this work.

type	δ -doping (cm $^{-2}$)	depth (Å)
p	3×10^{12}	80
		80
	3×10^{13}	150
		300
1×10^{14}	80	

by the band-bending value determined on a MBE-grown bulk n -type doped sample after decapping. In fact, analyzing the HREELS measurements by means of the dielectric model described below, we obtained a band bending of 0.63 eV, in excellent agreement with the literature value.²¹

HREELS measurements were performed at room temperature (RT) in specular geometry, with an angle of incidence of 65° and primary beam energies E_0 in the 2–50-eV range. The energy resolution was about 8 meV, as derived from the full width at half maximum (FWHM) of the elastic peak in the fitting procedure.

III. RESULTS

Figure 1 shows the spectra taken on three samples with different doping densities but the same dopant layer depth under the surface (80 Å). It can immediately be noted that the spectrum shape is strongly affected by the doping value. The spectra taken on the more lightly doped sample [3×10^{12} cm $^{-2}$, Fig. 1(a)] are characteristic of semi-intrinsic, i.e., undoped, GaAs. Indeed, besides the quasielastic (q - e) peak, the only visible loss structures are those due to the optical phonon at ~ 36 meV and its first overtone at ~ 72 meV, without any evidence of features due to a free-carrier gas.

Very different are the spectra taken on the sample doped 3×10^{13} cm $^{-2}$, shown in Fig. 1(b), where the q - e peak is strongly broadened. By increasing the primary energy from 2 to 50 eV, the full width at half maximum (FWHM) of the q - e peak decreases from ~ 60 to ~ 26 meV, values very large compared to the FWHM of the spectra relative to the more lightly doped sample (~ 11 meV). The optical phonon is almost completely screened, and is visible only as a weak shoulder on the q - e peak tail. Its feature can clearly be detected only at the highest primary energies, where the q - e peak is narrower. This behavior is, actually, the one expected on the basis of the kinematic of the electron scattering in the presence of an acoustical branch (see below).

Yet another behavior is presented by the spectra of the sample having the highest nominal doping [1×10^{14} cm $^{-2}$, Fig. 1(c)]. With respect to the previous one, the q - e peak is narrower and comparable to that of the more lightly doped sample (the FWHM is 14–19 meV), but with strong loss features. The most prominent one is centered at about 100 meV and is ~ 40 meV wide, superimposed on a strong and flat background, which achieves its maximum intensity at $E_0 = 5$ eV.

Turning now to the effect of the depth of the dopant layer on the HREEL spectra, Fig. 2 shows the spectra on three samples with the same doping value (3×10^{13} cm $^{-2}$), but with the charge layer placed respectively at 80, 150, and 300 Å under the surface. All the spectra are characterized by a pronounced broadening of the q - e peak, which decreases on increasing the primary energy, while the optical phonon is strongly screened. Both the broadening of the q - e peak and the phonon screening are less pronounced for increasing depths of the dopant layer, i.e., of the free-carrier gas.

IV. DATA ANALYSIS

A. Elementary excitations in a 2D electron gas

As recalled above, one of the fundamental differences between a 2D and 3D electron gas is the dispersion of the collective excitations. In a 3D electron gas (3DEG) the plasmon frequency attains a nonzero value in the long wavelength limit [$\omega_{\text{pl}}^2(3\text{D}) = 4\pi n_{3\text{D}} e^2 / m^* \epsilon_\infty$ as $q_{\parallel} \rightarrow 0$], while in a 2DEG it approaches zero¹⁷ [$\omega_{\text{pl}}^2(2\text{D})$

$= (2\pi n_{2\text{D}} e^2 / m^* \epsilon_\infty) q_{\parallel}$ as $q_{\parallel} \rightarrow 0$]. Here $n_{3\text{D}}$ ($n_{2\text{D}}$ is the 3D (2D) free-carrier density, m^* the effective mass, and q_{\parallel} the plasmon wave vector. Following the literature, in analogy to the bulk phonon spectra, we will indicate the dispersion behavior in the 3D and 2D cases as "optical" and "acoustical," respectively. Actually the term 2D should strictly indicate an ideal 2DEG, namely a sheet of charges having zero thickness and a single electronic band. A real 2DEG (quasi-2DEG) has a finite thickness and, usually, several occupied subbands, giving a complex

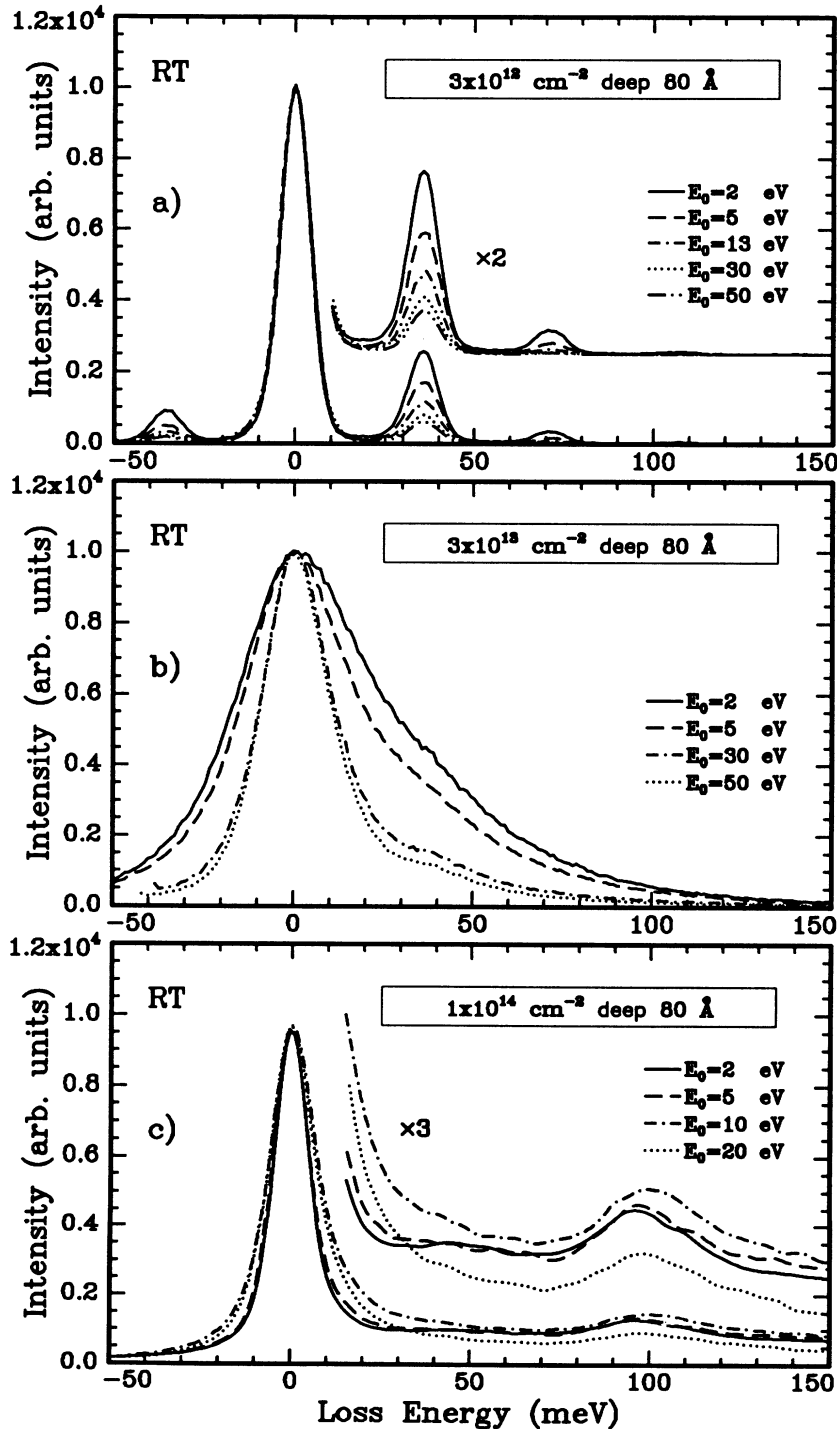


FIG. 1. HREEL spectra taken at different primary energies ($\Theta_i = 65^\circ$), on three samples p - δ doped (Be) where the dopant layer is placed 80 Å below the surface, and the nominal doping ranges from 3×10^{12} to 1×10^{14} cm^{-2} .

elementary excitation spectrum.²²⁻²⁴ Mills²³ and Yu and Hermanson²² calculated the HREEL scattering cross section for a real 2DEG (an accumulation layer of electrons in parabolic bands) based on the nonlocal dielectric response. They showed that, because of their relative HREEL scattering cross sections, the single-particle excitations and interband plasmons can be neglected with respect to the intraband plasmons. In the case of only two occupied subbands, the plasmon spectrum shows two branches with different dispersions: an upper one, whose energy is roughly proportional to $\sqrt{q_{\parallel}}$, and a lower one,

whose energy depends linearly on q_{\parallel} .²⁵⁻²⁷ The lower branch, however, exists only when the two populations are physically separated; otherwise the excitation rapidly decays into $e-h$ pairs (Landau damping) and does not appear as a well-defined spectral feature.²⁶ Moreover, Jain and Das Sarma²⁵ found that the finite thickness and coupling between subbands actually modify the dispersion of the upper branch with respect to the ideal 2D system ($\propto \sqrt{q_{\parallel}}$), but without changing it substantially.

As a consequence, in the analysis of our experimental results we can treat the free-carrier gas as an ideal one,

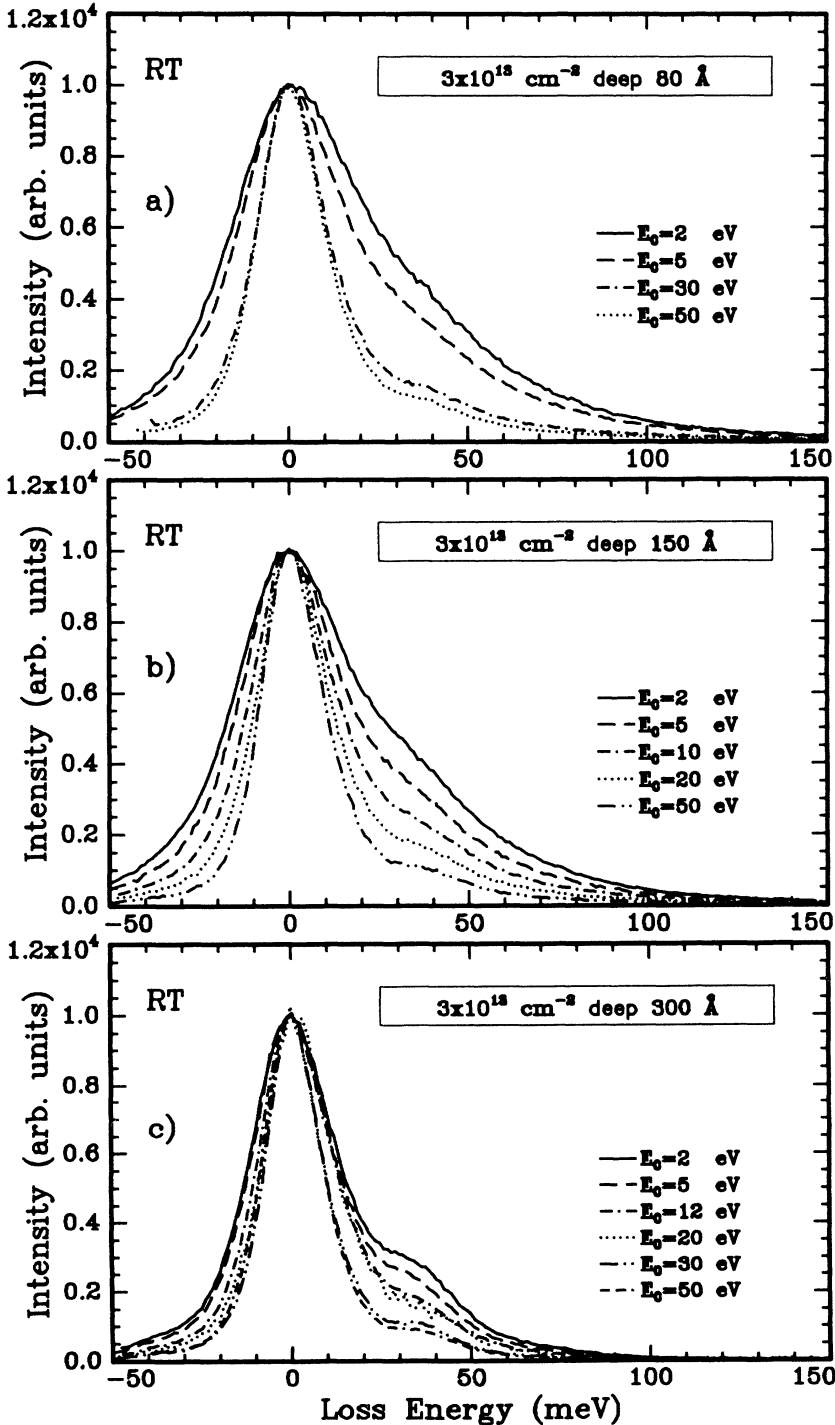


FIG. 2. HREEL spectra taken at different primary energies ($\Theta_i = 65^\circ$), on three samples p - δ -doped (BE) with the same dopant layer density ($3 \times 10^{13} \text{ cm}^{-2}$), placed, respectively, 80, 150, and 300 Å below the surface.

recalling, however, that the electronic structure of a p -type δ -doped system is more complicated than an n -type one,²⁸ due to the degeneration of two valence subbands at the Γ point of the Brillouin zone.

Besides the free-carrier collective excitation discussed above, in polar semiconductors the optical lattice vibrations also contribute to the dielectric response of the system. In particular, the plasmon can couple with the electric dipole moment associated with the longitudinal optical (LO) phonon to give the so-called plasmarons, collective excitations with mixed character. While one plasmaron has an acoustical dispersion behavior, similar to that of the 2D plasmon, the second one has an optical dispersion relation.²²

In synthesis, the excitations characterizing our quasi-2D system are the two plasmarons in the free-carrier region (δ -doped region), and the uncoupled optical phonon in the surface region without carriers.

In Fig. 3 are depicted the physical basis of a HREEL spectrum. Sketched in it are the dispersion relations of the plasmarons, for brevity indicated as optical and acoustical branches, and the HREEL kinematical curves (straight lines) relative to two different values of the primary beam energy. From the theory, it can be obtained that in specular geometry the dipole scattering cross section is expressed by the product of the kinematical factor (K_F) times the loss function (LF):²⁹

$$\frac{\partial^2 \sigma}{\partial \hbar \omega \partial \Omega} = K_F \text{Im} \left[\frac{-1}{1 + \epsilon_{\text{eff}}(q_{\parallel}, \omega)} \right], \quad (1)$$

$$K_F \propto \frac{q_{\parallel}}{[v_{\perp}^2 q_{\parallel}^2 + (\omega - \mathbf{q}_{\parallel} \cdot \mathbf{v}_{\parallel})^2]^2}.$$

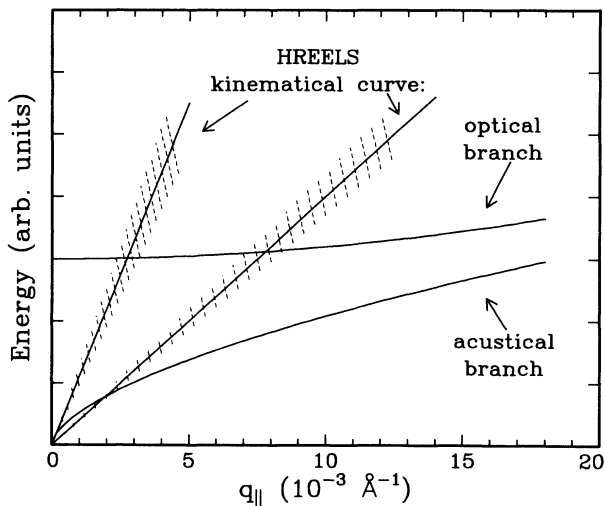


FIG. 3. Schematic illustration of the kinematical conditions in HREEL measurements of excitation having “optical” and “acoustical” dispersion relation. The straight lines are the so-called “kinematical straight lines,” deriving from the energy and momentum conservation in the scattering process. The intersection between the kinematical straight line and the dispersion relation curves corresponds to a feature in the HREEL spectrum (surf-riding condition). The shadowed area represent the region where the kinematical factor get values of the same order of magnitude of its local maximum.

The kinematical straight line is the locus of the points where K_F has its maximum value, corresponding to the so-called “surf-riding” condition ($\omega - \mathbf{q}_{\parallel} \cdot \mathbf{v}_{\parallel} = 0$). Its slope depends on the experimental parameters, that is the energy E_0 and the incidence angle Θ_I of the primary beam. The slope increases with both E_0 and Θ_I . The shadowed area represent the region where the kinematical factor is given values comparable to its local maximum. It follows, therefore, that the energy-loss features, for each E_0 , will occur at the intersections of the corresponding kinematical straight lines with the dispersion relation curves. The features are sharp and well defined when the branch is optical, and only a few modes can be excited in the region around the intersection, whereas in the case of the acoustical branch one can excite modes in a whole q_{\parallel} range $[0, q_{\parallel}^*]$. q_{\parallel}^* can be negligible, and then no feature associated with free carriers will appear in the spectrum. Otherwise q_{\parallel}^* can be finite, and then a large broadening of the quasielastic peak will occur.

B. Model calculations

From this situation described above the practical impossibility of deducing the properties of the acoustical plasmon in a 2D systems follows directly from the experimental HREEL spectra. The alternative approach is to calculate theoretical spectra based on a suitable model system and compare them to the experimental results, in order to deduce the characteristic dispersion and parameters of the system analyzed from the “best-fitting” spectra. However, also defining the theoretical model is not straightforward. A direct approach from first principles to the description of the nonlocal dielectric response of the real system is a very difficult task. Theoretical analysis of HREEL measurements taken on accumulation layers has been treated, until now, only numerically and in a quite complex way.^{22,23} A crude but much easier approach could be the use of a fictitious model able to reproduce the elementary excitations already discussed above, namely the plasmarons and the optical phonon. These requirements are met by a dielectric model consisting in a thin 3DEG, that is a thin layer [of thickness d_2 and background dielectric function $\epsilon_2(\omega)$] containing a carrier gas of density n , sandwiched between a semi-infinite substrate (the bulk) on one side and a layer of thickness d_1 in contact with the vacuum (the depleted layer) on the other side, both with a background dielectric function $\epsilon_1(\omega)$. The dielectric response of the sandwiched carrier gas can be described by the Drude term $-\omega_{\text{pl}}^2 / \omega(\omega - i\gamma_{\text{pl}})$. The plasma frequency is $\omega_{\text{pl}}^2 = 4\pi e^2 [n_{3\text{D}}^{\text{hh}} / m_{\text{hh}}^* + n_{3\text{D}}^{\text{lh}} / m_{\text{lh}}^*]$, where $m_{\text{hh},\text{lh}}^*$ is the effective mass of the hole in the crystal and γ_{pl} is the plasmon damping. This is the same approach used in the description of heavily doped p -type bulk GaAs,³⁰ where we showed that the dielectric response of a two-component hole gas (heavy and light) is described by a single Drude term.

The dielectric theory^{19,31,29} allows us to obtain the dispersion of the collective excitations of the whole system having two branches, one with optical character and the other with acoustical character. In other words, in

the limit of “thin gas,” that is $q_{\parallel}d_2 \ll 1$, the confinement of a classical carrier gas produces an electron collective excitation having acoustical dispersion¹⁹ which coincides with the plasma excitation of an ideal 2D electron gas. This model, however, also predicts an optical branch with a downward dispersion, the opposite of what is expected for the optical plasmaron branch of a “true” 2DEG.²²

In spite of the strong approximations intrinsic in the use of this dielectric model, reproducing the HREEL spectra, at least the part near the q - e peak, can still provide important information about the behavior and properties of the free-carrier gas.

HREEL spectra calculations were carried out starting from the above-described model by means of the Lambin code,³² able to simulate a complete HREEL spectrum through the computation of the effective dielectric function $\epsilon_{\text{eff}}(\omega)$ of a system composed of different layers, once given the layer thickness d_i and its dielectric function $\epsilon_i(\omega)$.

In our case two layers, the depleted region and the bulk, are characterized by the simple lattice vibration (phonon), described by a Lorentz oscillator term, added to the background electronic contribution in the infrared region ϵ_{∞} :

$$\epsilon_{\text{bulk}}(\omega) = \epsilon_{\infty} + \frac{(\epsilon_0 - \epsilon_{\infty})\omega_{\text{TO}}^2}{\omega_{\text{TO}}^2 - \omega^2 - i\omega\gamma_{\text{ph}}}, \quad (2)$$

with $\omega_{\text{TO}} = 33.41$ meV, $\gamma_{\text{ph}}/\omega_{\text{TO}} = 0.009$ and $\epsilon_{\infty} = 10.91$, $\epsilon_0 = 12.91$.³³ The dielectric function of the thin layer, the classically confined free-carrier gas, is obtained by adding to $\epsilon_{\text{bulk}}(\omega)$ a Drude term $\epsilon_{\text{pl}}(\omega)$, determined by the unscreened plasma frequency $\omega_{\text{pl}}^2 = 4\pi n e^2 / m^*$. Therefore

$$\epsilon_{\text{EG}}(\omega) = \epsilon_{\infty} + \frac{(\epsilon_0 - \epsilon_{\infty})\omega_{\text{TO}}^2}{\omega_{\text{TO}}^2 - \omega^2 - i\omega\gamma_{\text{ph}}} - \frac{\omega_{\text{pl}}^2}{\omega(\omega + \gamma_{\text{pl}})}, \quad (3)$$

where ω_{pl} and γ_{pl} are the plasmon energy and damping parameter.

V. DISCUSSION

The calculated spectra in better agreement with experimental ones relative to the more lightly doped sample correspond to a semi-infinite undoped GaAs substrate (Fig. 4). This result comes from the lack of features due to a free-carrier gas, and this is what is expected for a low doping level. In fact, since the 2D-plasmon energy is proportional to the square root of the surface density of free carriers, when the free carrier concentration is very low the intersection between the kinematic straight line and the dispersion curve is in practice limited to the $q \simeq 0$ point; thus there is no broadening of the q - e peak, nor any other feature, exactly as if the sample did not contain free carriers. Actually, we expected this behavior only at doping levels lower than the actual one. In fact, simulations performed by using the thin-gas dielectric model and assuming the bulk effective masses of the heavy ($m_{\text{hh}}^* = 0.45m_0$) and light ($m_{\text{lh}}^* = 0.082m_0$) holes, indicate that in GaAs HREELS could detect hole densities

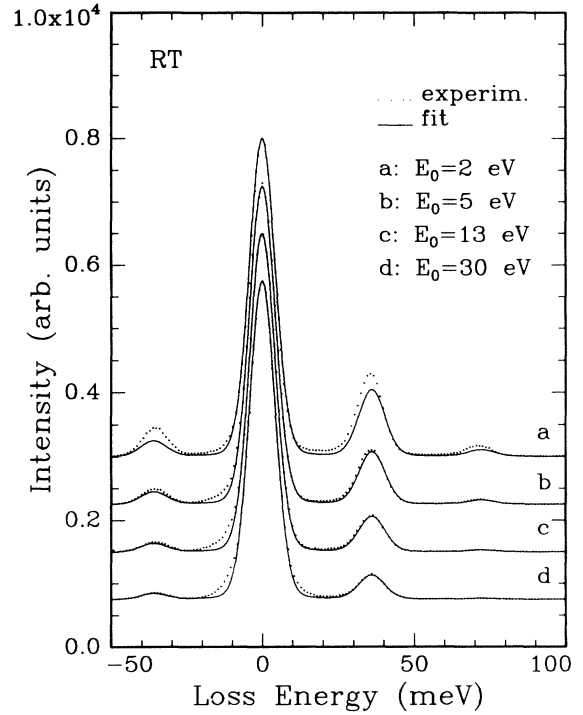


FIG. 4. Experimental spectra (points) for the sample nominally doped $3 \times 10^{12} \text{ cm}^{-2}$ with the dopant placed 80 \AA below the surface. Theoretical spectra calculated using the “thin gas” dielectric model (see text), assuming a doping level below $3 \times 10^{12} \text{ cm}^{-2}$.

down to $8 \times 10^{11} \text{ cm}^{-2}$. We will discuss this point below later.

Figure 5 shows the experimental and calculated spectra superimposed relative to the sample $3 \times 10^{13} \text{ cm}^{-2}$ – 80 \AA . Since the order of magnitude of the typical excitation wave vector, q_{\parallel} , is 10^{-2} \AA^{-1} , we assumed the gas layer thickness d_2 equal to 5 \AA to fulfill the “thin” gas condition ($q_{\parallel}d_2 \ll 1$). We recall here that this value has no connection with the extension of the electronic wave function in the real system, because the “thin gas” is only a way to simulate (almost exactly), the ideal 2D behavior of the free-carrier gas. The spectra in the figure were obtained by finding the best fit to the spectrum with $E_0 = 5$ eV, adjusting the thickness of the depleted layer (d_1), the unscreened plasma frequency γ_{pl} and the plasmon damping (ω_{pl}), and then searching for their best fit at all other primary energies, changing only the plasmon damping. They are in fairly good agreement with experiments. In a similar way, spectra relative to the sample with the same doping but with different depth of the dopant sheet also could be “fitted.” For the sake of simplicity, we do not show them.

We also tried to reproduce the spectra by a dielectric model similar to the one just described, but with a “thick” free-carrier gas; that is, with the free-carrier gas having a thickness comparable to the z extension of the hole wave function (several hundreds \AA), assumed to show a 3D behavior. In this case the best fit gave a poorer agreement with experimental spectra, and less reason-

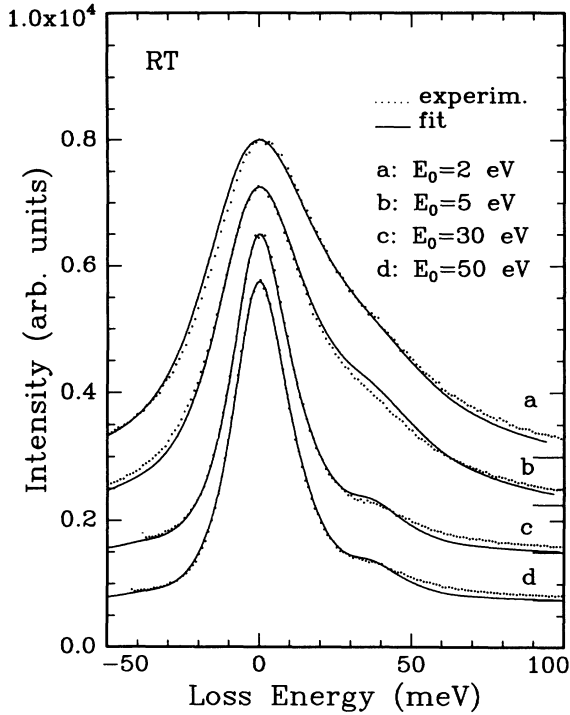


FIG. 5. Experimental (points) and theoretical (solid line) spectra calculated by using the “thin gas” dielectric model (see text), for the sample doped $3 \times 10^{13} \text{ cm}^{-2}$ with the dopant placed 80 Å below the surface. The model parameters are shown in Table II.

able parameters. Our results clearly show the expected 2D behavior of the hole gas produced in GaAs by a δ -doping of $3 \times 10^{13} \text{ cm}^{-2}$. The parameters we obtained from the best-fit procedure are shown in Table II.

From the plasma frequency this obtained, $\hbar\omega_{\text{pl}} = 653 \text{ meV}$, we can extract the surface density of the hole gas.

TABLE II. Parameters obtained from the best agreement between experimental and calculated spectra.

Depth (Å)	E_0 (eV)	γ_{pl}	d_1 (Å)	ω_{pl} (meV)
80	2	41.0	47	653
	5	34.2		
	30	10.5		
	50	5.4		
150	2	36.7	64.2	653
	5	31.4		
	10	25.4		
	20	16.8		
	50	6.6		
300	2	44.1	163.3	
	5	31.2		
	12	18.0		
	20	12.3		
	30	13.2		
	50	7.2		

In fact, assuming that the sharing between heavy and light holes and the effective masses are the same as in the bulk, we find a hole surface density of $\approx 0.7 \times 10^{13} \text{ cm}^{-2}$, a value well below the nominal doping. Together with the result for the more lightly doped sample, this is a further indication of the underestimation (by a factor 4–5) of the free carrier surface density as derived from the plasma frequency obtained from the best fit. This can be attributed to two possible effects: (i) a free-carrier trapping, connected to the intrinsic band-bending at the (100) surface¹⁹ and/or (ii) a different in-plane effective mass of the holes. In a p -type δ -doped system, in fact, the electronic structure is quite complex: due to the strong intermixing between heavy and light subbands, their dispersion is highly nonparabolic and show unexpected features.^{34,28} In particular, the value of the in-plane effective masses (m_{\parallel}^*) is different from the bulk ones, provided this parameter has still some meaning. Therefore, only a calculation of the plasma frequency starting from the detailed band structure of the system could allow one to extract the real relation between ω_{pl} and the free-carrier concentration.

An interesting feature shown by the plasma damping γ_{pl} is its strong dependence on the primary energy, a behavior similar to what is found in bulk p -type GaAs(110),³⁰ and ascribed to the Landau damping of the collective free-carrier excitation. An analysis in this direction is underway, and its results will be presented separately.

Finally let us discuss the results obtained on the highest doped sample ($1 \times 10^{14} \text{ cm}^{-2}$). The spectra calculated within the “thin-gas model” [Fig. 6(a)] show a strong dependence on the primary energy E_0 , as expected from the scattering kinematics depicted in Fig. 3. The experiments, on the contrary, show a plasmon feature whose position depends only slightly on E_0 [see Fig. 1(c)]. This last characteristic is proper of an “optical” plasmon in a 3D system, therefore we tried to reproduce these experimental data by assuming a “thick” gas layer. As can be seen in Fig. 6(b), the HREEL spectra calculated within the “thick” (3D) gas model are in much better agreement with the experiment; in particular, the plasmon intensity dependence on E_0 is well reproduced. The parameters used to fit the spectra are the layer width $d_2 = 400 \text{ Å}$ and $\omega_{\text{pl}} = 400 \text{ meV}$ (corresponding to a surface density of $1.5 \times 10^{14} \text{ cm}^{-2}$). The plasmon damping γ_{pl} was found to be 50 meV, comparable to the typical value found on heavily p -type-doped bulk GaAs.³⁰ Actually, at this high doping level, the dopant atoms are probably diffused over several hundred Å and, therefore, the potential well is also quite broad. Since the free carriers are holes, their effective mass is high and the occupied subbands will be numerous and very close to one another; therefore, it is reasonable that in this condition the 2D \rightarrow 3D transition has already occurred and therefore it is correct to find a 3D behavior of the hole gas.¹⁵

In summary, we found that the samples with the two lowest dopings show a quasi-2D behavior, whereas the sample with the highest doping shows characteristic properties of a 3D free-carrier gas.

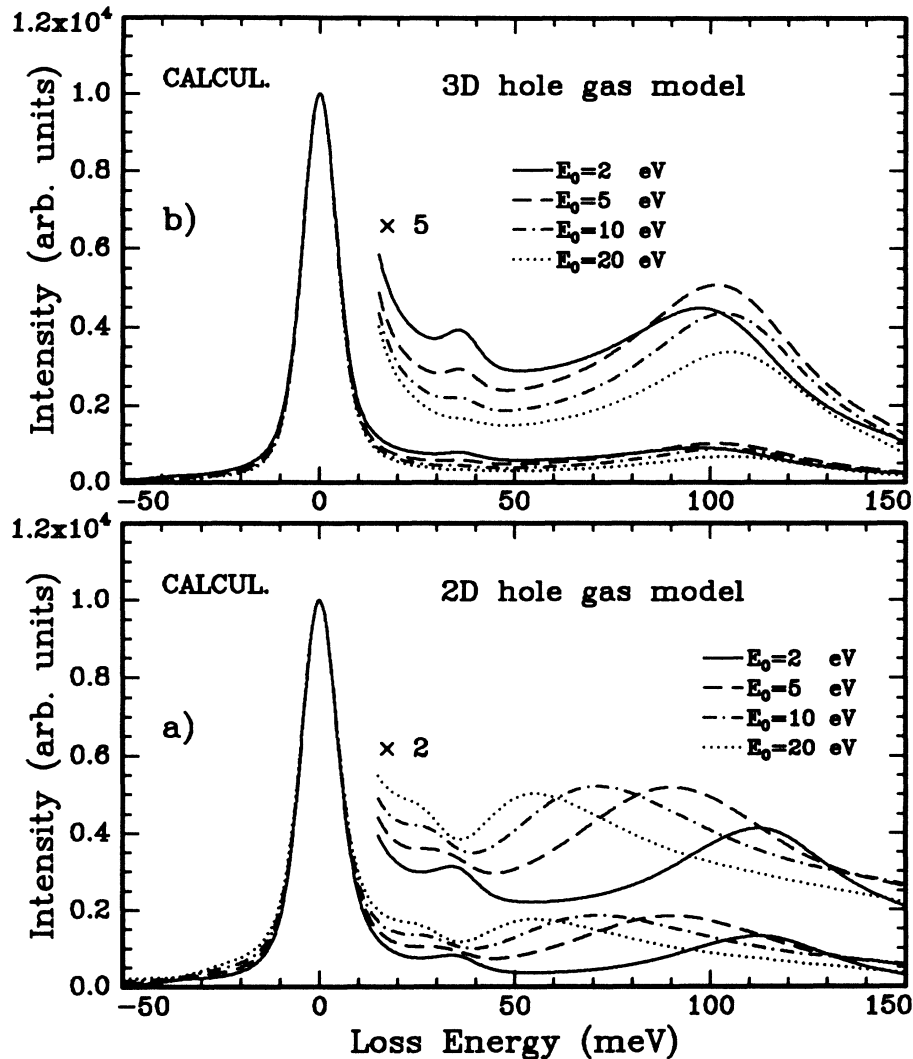


FIG. 6 HREEL spectra calculated by means of a dielectric model of a free-carrier gas classically confined in the limit of “thin gas” (a) and “thick gas” (b) for the sample doped 1×10^{14} . The model parameters are the following: (a) $d_1 = 15 \text{ \AA}$, $d_2 = 5 \text{ \AA}$, $\omega_{pl} = 1400 \text{ meV}$, and $\gamma_{pl} = 10 \text{ meV}$. (b) $d_1 = 10 \text{ \AA}$, $d_2 = 400 \text{ \AA}$, $\omega_{pl} = 400 \text{ meV}$, and $\gamma_{pl} = 50 \text{ meV}$.

VI. CONCLUSIONS

We have presented a HREELS investigation of the low-energy excitations of δ -doped p -type GaAs(001) samples, with three levels of doping. We have shown that the charge density of the doping layer and its depth under the surface strongly affects the spectra. All experimental spectra could be reproduced by the use of the suited dielectric model. The more lightly doped sample ($3 \times 10^{12} \text{ cm}^{-2}$) appears as undoped, while samples with intermediate doping ($3 \times 10^{13} \text{ cm}^{-2}$) show spectra with a large broadening of the quasielastic peak and an almost complete screening of the surface optical phonon, without any other evident features. Both sets of spectra could be well reproduced by means of the dielectric model of a classically confined free-carrier gas, in the limit of “thin gas,” which reproduces almost exactly the behavior of an ideal 2D free-carrier gas. Conversely, in the spectra of the most doped samples ($1 \times 10^{14} \text{ cm}^{-2}$), a narrower quasielastic peak and a well-defined loss structure appear. The largest loss feature is attributed to a plasma excitation with a well-defined 3D character, reasonably because

of the large number of occupied subbands in the potential well produced by the doping layer.

The effect of the depth of the dopant layer has also been investigated. This parameter affects the spectral shape, but in a way that could be satisfactorily reproduced by the dielectric model.

ACKNOWLEDGMENTS

The samples used in the present studies were supplied by Laboratorio Tecnologie Avanzate Superfici e Catalisi—Consorzio Interuniversitario Nazionale di Fisica della Materia (TASC-INFM), Area di Ricerca, Padriciano 99, I-34012 Trieste, Italy. We thank in particular L. Sorba, G. Bratina, G. Biasiol, R. Nicolini, and A. Franciosi of the TASC staff. Annalisa Fasolino, Carlo Mariani, and Maria Grazia Betti are warmly thanked for helpful discussions. We thank E. Angeli for the invaluable experimental assistance. Financial support from Italian Ministero dell’Università e della Ricerca Scientifica e Tecnologica (MURST) is also acknowledged.

- ¹T. Ando, A. B. Fowler, and F. Stern, *Rev. Mod. Phys.* **54**, 437 (1982).
- ²M. Jaros, *Physics and Applications of Semiconductor Microstructures* (Clarendon, Oxford, 1989).
- ³A. Many, I. Wagner, A. Rosenthal, J. I. Gersten, and Y. Goldstein, *Phys. Rev. Lett.* **46**, 1648 (1981).
- ⁴J. I. Gersten, I. Wagner, A. Rosenthal, Y. Goldstein, A. Many, and R. E. Kirby, *Phys. Rev. B* **29**, 2458 (1984).
- ⁵Y. Chen, J. C. Hermanson, and G. J. Lapeyre, *Phys. Rev. B* **39**, 12 682 (1989).
- ⁶L. Bu, Y. Zhang, B. A. Mason, R. E. Doezema, and J. A. Slinkman, *Phys. Rev. B* **45**, 11 336 (1992), and bibliography therein.
- ⁷M. Noguchi, K. Hirakawa, and T. Ikoma, *Phys. Rev. Lett.* **66**, 2243 (1991).
- ⁸E. F. Schubert, *J. Vac. Sci. Technol. A* **8**, 2980 (1990).
- ⁹E. F. Schubert, J. B. Stark, B. Ullrich, and J. E. Cunningham, *Appl. Phys. Lett.* **52**, 1508 (1988).
- ¹⁰A. Zrenner, F. Koch, and K. Ploog, *Surf. Sci.* **196**, 671 (1988).
- ¹¹R. B. Beall, J. B. Clegg, and J. J. Harris, *Semicond. Sci. Technol.* **3**, 612 (1988).
- ¹²A. M. Lanzillotto, M. Santos, and M. Shayegan, *Appl. Phys. Lett.* **55**, 1445 (1989).
- ¹³M. H. Degani, *Phys. Rev. B* **44**, 5580 (1991).
- ¹⁴A. Zrenner, F. Koch, R. L. Williams, R. A. Stradling, K. Ploog, and G. Weimann, *Semicond. Technol.* **3**, 1203 (1988).
- ¹⁵D. A. Poole, M. Pepper, K. F. Bergreen, G. Hill, and H. W. Myron, *J. Phys. C* **15**, L21 (1982).
- ¹⁶B. E. Sernelius, K. F. Bergreen, M. Tomak, and C. McFadens, *J. Phys. C* **18**, 225 (1985).
- ¹⁷F. Stern, *Phys. Rev. Lett.* **18**, 546 (1967).
- ¹⁸A. Mooradian, in *Light Scattering Spectra of Solids*, edited by G. B. Wright (Springer-Verlag, Berlin, 1968).
- ¹⁹C. Lohe, A. Leuther, A. Föster, and H. Lüth, *Phys. Rev. B* **47**, 3819 (1993).
- ²⁰Y. Chen, S. Nannarone, J. Schaefer, J. C. Hermanson, and G. J. Lapeyre, *Phys. Rev. B* **39**, 7653 (1989).
- ²¹W. Chen, M. Dumas, D. Mao, and A. Kahn, *J. Vac. Sci. Technol. B* **10**, 1886 (1992).
- ²²Y. Chen, J. C. Hermanson, and G. J. Lapeyre, *Phys. Rev. B* **39**, 12 682 (1989); H. Yu and J. C. Hermanson, *ibid.* **40**, 11 851 (1989); **41**, 5991 (1990).
- ²³D. H. Ehlers and D. L. Mills, *Phys. Rev. B* **36**, 1051 (1987); S. R. Streight and D. L. Mills, *ibid.* **40**, 10 488 (1989).
- ²⁴E. Burnstein, A. Pinczuk, and D. L. Mills, *Surf. Sci.* **98**, 451 (1980).
- ²⁵J. K. Jain and S. Das Sarma, *Phys. Rev. B* **36**, 5949 (1987).
- ²⁶G. E. Santoro and G. F. Giuliani, *Phys. Rev. B* **37**, 937 (1988).
- ²⁷E. Batke, D. Heitmann, and C. W. Tu, *Phys. Rev. B* **34**, 6951 (1986).
- ²⁸F. A. Reboredo and C. R. Proetto, *Phys. Rev. B* **47**, 4655 (1993).
- ²⁹H. Ibach, and D. L. Mills, *Electron Energy Loss Spectroscopy and Surface Vibrations* (Academic, New York, 1982).
- ³⁰R. Biagi, Carlo Mariani, and U. del Pennino, *Phys. Rev. B* **46**, 2467 (1992).
- ³¹Ph. Lambin, J. P. Vigneron, and A. A. Lucas, *Phys. Rev. B* **32**, 8203 (1984).
- ³²Ph. Lambin, J. P. Vigneron, and A. A. Lucas, *Comput. Phys. Commun.* **60**, 351 (1990).
- ³³Z. T. J. Gray-Grychowsky, R. G. Egdell, B. A. Joyce, R. A. Stradling, and K. Woodbridge, *Surf. Sci.* **186**, 482 (1987).
- ³⁴M. Altarelli, U. Ekenberg, and A. Fasolino, *Phys. Rev. B* **32**, 5138 (1985).